PROPOSED POWER OPTIMIZATION FOR UPLINK MULTI-ARS SMALL-CELL COMMUNICATION NETWORK

Võ Quang Dũng*, Ngô Thanh Tùng
Trường Đại học Thông tin liên lạc

Thông tin chung:
Ngày nhận bài: 9/01/2025
Ngày phản biện: 11/01/2025
Ngày duyệt đăng: 27/02/2025
**Tác giả chính:*
voquangdung.sqtt@gmail.com
DOI:
https://doi.org/10.70879/8QE9ZJlEd

Title:
Đề xuất bài toán tối ưu hóa công suất cho truyền thông đường lên trong mạng tế bào nhỏ đa-ARS, mạng không phân chia tế bào, điều khiển công suất.

Từ khóa:
Tế bào nhỏ, trạm chuyển tiếp trên không, tối ưu công suất.

Keywords:
Small Cell, aerial relay stations , power optimization, cell free network, power contol.

TÓM TẮT*: Các mô hình tế bào nhỏ (SC: Small Cell) và thiết bị bay không người lái (UAV: unmanned aerial vehicles) hoạt động như các trạm chuyển tiếp trên không (ARS: aerial relay stations) được xem là những bước tiến hứa hẹn cho mạng không dây thế hệ mới, góp phần nâng cao chất lượng dịch vụ. Nghiên cứu này tập trung vào mô hình không phân chia tế bào (CF: cell free) sử dụng nhiều ARS, trong đó một số lượng lớn ARS được phối hợp bởi trạm gốc mặt đất (GBS) và cùng nhau phục vụ nhiều người dùng thông qua việc chia sẻ tài nguyên tần số và thời gian. Mô hình SC được thiết kế sao cho mỗi người dùng được phục vụ bởi một ARS duy nhất, được chọn thông qua thuật toán lựa chọn ARS. Biểu thức dạng đóng của thông lượng người dùng đường lên được xây dựng, và tối ưu hóa công suất được đề xuất sử dụng thuật toán Bisection. Đánh giá hệ thống thông qua hàm phân phối tích lũy (CDF:cumulative distribution functions) của thông lượng người dùng cho thấy rằng việc lựa chọn ARS giúp giảm độ phức tạp, trong khi đó bài toán tối ưu hóa công suất cải thiện đáng kể thông lượng.*

ABSTRACT*: Small Cell (SC) frameworks and unmanned aerial vehicles (UAVs) functioning as aerial relay stations (ARSs) represent promising advancements for next-generation wireless networks, enhancing service quality. This study focuses on the Multi-ARS Cell-Free (CF) framework, which eliminates cell boundaries, wherein a substantial number of ARSs are coordinated by the ground base station (GBS) and collaboratively serve numerous users using shared frequency and time resources. The SC model is designed such that each user is served by a single ARS selected through the ARS selection algorithm. A closed-form expression for uplink user throughput is derived, and power optimization is proposed using the Bisection algorithm. System evaluation via cumulative distribution functions (CDFs) of user throughput demonstrates that ARS selection reduces complexity, while power optimization significantly enhances throughput.*

1. Introduction

Wireless technology has experienced remarkable progress since its inception. Its future appears bright with advancements such as 5G networks, the Internet of Things (IoT), and artificial intelligence (AI). Modern communication frameworks enable a significant increase in connected devices,

deliver high-speed data transmission, and achieve near real-time responsiveness [1]. The rapid evolution and global adoption of 5G have paved the way for designing wireless technologies beyond 5G (B5G), demanding unprecedented network density and higher mobile data consumption. To address these challenges, Small Cell (SC) architectures are being explored to enhance coverage and capacity in densely populated urban areas[2].

SC architectures comprise low-power cellular access nodes that are integral to the design of 5G wireless networks. These nodes are engineered to improve network coverage and capacity in areas with high traffic demand or inadequate signal strength. Compared to traditional cellular towers, SC are more cost-efficient, occupy less physical space, and consume less power [3]. Pak et al. [4] analyzed effective SC deployment scenarios, focusing on signal-to-interference-plus-noise ratio (SINR) outcomes. However, deployment complexity increases due to cross-cell interference (between macrocells and small cells) and inter-cell interference, which pose major challenges for SC implementation [5]. Additionally, SC models face significant issues related to handovers between cells. To address these challenges, 5G mobility management in ultra-dense small cell networks, particularly handover optimization using reinforcement learning techniques, has been studied, offering targeted solutions to these problems [6].

Due to their capability to function at elevated altitudes and adjust to dynamic environmental factors, ARS systems provide an exceptional framework for improving wireless network performance and delivering a smooth, high-quality user experience. The use of ARSs enhances both spatial and time diversity in wireless signals. Combining ARS communication with SC models presents a promising approach for improving coverage and service quality in high-mobility scenarios, offering an innovative advancement for the communications technology sector [7].

Current cellular base stations lack flexibility and mobility. To address this, ARS communication has emerged as a promising solution, offering benefits such as cost efficiency, wide coverage, reliable coordination with ground devices, and a robust backup network. ARSs outperform terrestrial relay stations in many scenarios due to their mobility and ability to reach inaccessible locations, improving Line-of-Sight (LoS) probability [8]. Key aspects like deployment, performance, resource management, trajectory optimization, and channel modeling have been extensively studied [9]. A stochastic geometry framework has also been proposed to analyze downlink coverage and ergodic capacity in ARS-assisted millimeter-wave networks [10].

1.1. Motivation

To the best of our knowledge, when surveying the SC and ARS models, it has been observed that combining these technologies presents a promising new research direction with significant practical potential for several reasons:

Firstly, while traditional SC models are effective in enhancing system performance, they face challenges such as cell-to-cell handovers and high interference when the number of small cells increases. These issues highlight the need for a more flexible approach to network design, moving away from the traditional "cell" concept.

Secondly, integrating ARSs with the SC model is an emerging area of research that remains relatively underexplored, particularly the development of a new SC model that eliminates the "cell" concept, such as in Cell-Free (CF) models. The combination of ARS

and SC technologies could create a novel model with key advantages, such as a higher likelihood of Line-of-Sight (LoS) communication, flexible deployment, and more efficient signal processing.

Finally, optimizing transmit power in a CF and SC system with multiple ARSs is essential for ensuring stable connectivity, reducing interference, and improving spectral efficiency. Effective power allocation enhances energy efficiency and prolongs network lifespan, addressing key challenges in ARS-based communication.

1.2. Contribution

The key contributions of this paper are outlined as follows:

We propose an uplink SC model built on the Cell-Free (CF) system [11, 12] where each user is assigned to a single ARS. The ARSs select users according to the best channel conditions to ensure efficient communication.

We develop the channel model based on the standards for Enhanced LTE Support for aerial vehicles set by the International Telecommunication Union (ITU) and the 3rd Generation Partnership Project (3GPP) [13]. The time division duplex (TDD) protocol is utilized, and the uplink channel is estimated using the Minimum Mean Square Error (MMSE) technique.

We derive a closed-form expression for the uplink throughput of the system and propose a strategy to optimize the uplink power coefficient via bisection method.

We assess the system's performance by comparing the user throughput with/without optimization. This analysis considers the influence of various system parameters, such as the number of ARSs, the number of antennas per ARS, the user count, and the length of the pilot sequences.

The structure of the paper is as follows: Section 2 introduces the SC multi-ARS system model. The uplink data transmission and ARS selection issues are addressed in Section 3. Section 4 focuses on the optimization of uplink power. Numerical results and related discussions are provided in Section 5, while the conclusion is presented in Section 6. For convenience, the mathematical notations are summarized in Table 1.

Table 1: The mathematical notation presented in this paper.

Parameter	Value
$\|\|.\|\|$	Euclidean norm
$(.)^{\mathrm{H}}$	Conjugate transpose
$(.)^*$	Conjugate
$\mathbb{E}\{.\}$	Expectation operator
I_N	The $N \times N$ identity matrix
$\mathbb{C}^{m \times n}$	Size of a vector or matrix
η_k^{u}	Data power control coefficient
η_k	Pilot power control coefficient
K	Number of users
M	Number of antennas at ARS
A	Number of ARSs

2. System Model

2.1. Channel Model

We initiate the deployment of the Multi-ARS CF system with A ARSs and K terrestrial users, as depicted in Figure 1. Each ARS is equipped with M antennas, while each user is equipped with a single antenna. The system is located in a large area of S km^2, with ARSs and users randomly positioned.

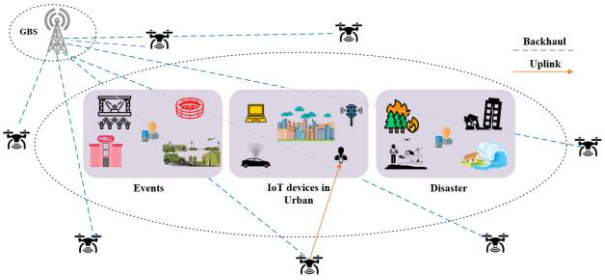

Figure 1: The system model of multi-ARS SC.

Furthermore, the ARSs are connected to the ground base station (GBS) via an ideal backhaul with infinite capacity.

The TDD protocol is employed as the foundation for network communication [14]. The coherence interval is divided into four phases: uplink training, uplink data transmission, downlink training, and downlink data transmission, as illustrated in Figure 2. Additionally, the framework assumes that all ARSs concurrently serve users by sharing the same time-frequency resources efficiently. Various strategies can be employed to determine the active set of ARSs, tailored to the specific requirements of the network.

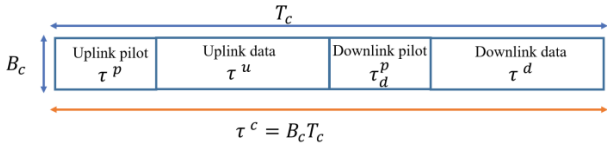

Figure 2: Time-division duplex protocol.

The propagation channel is influenced by two main components: small-scale fading and large-scale fading. In scenarios where ARSs operate at significant altitudes, large-scale fading is predominantly determined by path loss. Within a single coherence interval, small-scale fading is assumed to be stable but varies independently across different intervals. Conversely, large-scale fading evolves at a much slower pace, remaining unchanged over multiple coherence intervals.

In this study, the channel coefficient vector describing the link between the *a*-th ARS and the *k*-th user is denoted as $\boldsymbol{g}_{ak} \in \mathbb{C}^{M\times 1}$. The expression for this channel coefficient vector is formulated as follows

$$\boldsymbol{g}_{ak} = \sqrt{\beta_{lk}}\boldsymbol{h}_{ak}, \qquad (1)$$

where, β_{ak} represents the coefficient for large-scale fading, while $\boldsymbol{h}_{ak} \in \mathbb{C}^{M\times 1}$ denotes the small-scale fading vector. The components of $\boldsymbol{h}_{ak}$ are independent and identically distributed (i.i.d.) random variables following a complex Gaussian distribution $\mathcal{CN}\left(0,\mathbf{I}_M\right)$.

The coefficient β_{ak} is influenced by the path loss occurring between the ARS and the corresponding user. The expression for the large-scale fading coefficient is formulated as follows:

$$\beta_{ak} = 10^{\frac{\mathrm{PL}_{ak}}{10}}, \qquad (2)$$

where PL_{ak} represents the path loss expressed in decibels. In this study, the evaluation of PL_{ak} is conducted under the Urban Micro (UMi) setting, following the guidelines outlined in the 3GPP specifications for aerial vehicle communications, as detailed in [13].

$$\mathrm{PL}_{lk} = max\left(\mathrm{PL}', \mathrm{PL}_{\mathrm{LoS}}, \mathrm{PL}_{\mathrm{NLoS}}\right) \qquad (3)$$

where, $\mathrm{PL}', \mathrm{PL}_{\mathrm{LoS}}, \mathrm{PL}_{\mathrm{NLoS}}$ represent the free-space path loss, LoS, and NLoS, respectively, which are expressed by the following expressions:

- $\mathrm{PL}' = -20\log_{10}\left(4\pi d_1\right) - 20\log_{10}\left(\frac{f_c}{3\times 10^8}\right)$,
- $\mathrm{PL}_{\mathrm{LoS}} = -30.9 - \left(22.25 - 0.5\log_{10}\left(h_{ARS}\right)\right)$ $\times\log_{10}\left(d_1\right) - 20\log_{10}\left(f_c\right)$,
- $\mathrm{PL}_{\mathrm{NLoS}} = -32.4 - \left(43.2 - 7.6\log_{10}\left(h_{ARS}\right)\right)$ $\times\log_{10}\left(d_1\right) - 20\log_{10}\left(f_c\right)$,

f_c represents the carrier frequency, measured in MHz. The height of the ARS is h_{ARS} with $22.5m \le h_{ARS} \le 300m$ and the distance between the ARS and the user is d_1.

Remark 1: The ARSs-based communication system outperforms ground node-based CF models due to consistently

available LoS links and negligible shadow fading. Its flexible deployment makes it ideal for scenarios like search and rescue, smart cities, or disaster recovery. Additionally, the multi-ARS SC model offers greater energy efficiency, reduced backhaul overload risk, and simpler ARS selection, power optimization, and signal processing compared to the multi-ARS CF model.

2.2 Multi-ARS Small Cell

The CF model with multiple ARSs allows all ARSs to serve users in a region without being limited by cell boundaries. The SC system is developed based on the CF framework, with the assumption that each user will be served by the best ARS, meaning the ARS with the strongest channel conditions, selected based on large-scale fading criteria. The mathematical model for the multi-ARS SC system is defined as follows:

$$k_a \triangleq \max_{k \in \{available\ users\}} \beta_{ak}. \quad (4)$$

The ARS selection method outlined above is relatively straightforward, achieving local optimization at each ARS. Effectively solving the ARS selection issue simplifies the design for signal processing and power control. This approach focuses on creating a flexible SC framework that performs effectively across diverse scenarios and supports rapid deployment. However, global optimization remains a challenge, as the outcome largely depends on the sequence in which ARSs choose users.

2.3 Uplink Communication

In the uplink, ARSs perform channel estimation by leveraging pilot signals sent by users. The MMSE method [15] is applied to detect these signals during the uplink training stage. In this process, all users transmit their pilot sequences simultaneously to the ARSs, which then process the received data to estimate the channel coefficients. These estimates are subsequently utilized to extract the desired signals. The pilot sequence of the k-th user is denoted as $\boldsymbol{\phi}_k \in \mathbb{C}^{\tau^{\mathrm{p}} \times 1}$,with the condition $\left\|\boldsymbol{\phi}_k\right\|^2 = 1 \forall k$.

The channel coefficients resulting from the MMSE estimation procedure can be written as

$$\hat{\boldsymbol{g}}_{ak_a} = \boldsymbol{g}_{ak_a} - \varepsilon_{ak_a}, \quad (5)$$

In this case, ε_{ak_a} represents the channel estimation error vector. According to the properties of MMSE estimation, ε_{ak_a} is uncorrelated with the estimated channel coefficients $\hat{g}_{ak_a}$. Furthermore, each element of the estimated channel vector $\hat{g}_{ak_a}$ follows a distribution of $\mathcal{CN}\left(0,\omega_{ak_a}\right)$, while each element of ε_{ak_a} is distributed as $\mathcal{CN}\left(0,\beta_{ak_a} - \omega_{ak_a}\right)$, where

$$\omega_{ak_a} \triangleq \frac{\tau^{\mathrm{p}} \rho^{\mathrm{p}} {\beta^2}_{ak_a}}{\tau^{\mathrm{p}} \rho^{\mathrm{p}} \sum_{a'=1}^{A} \beta_{ak_{a'}} \left\|\boldsymbol{\phi}_{k_a}^H \boldsymbol{\phi}_{k_{a'}}\right\|^2 + 1}. \quad (6)$$

Denote ρ^{u} represent the normalized uplink SNR, and $\eta_{k_a}^{\mathrm{u}}$ denote the power control coefficient for the k_a th user with $0 < \eta_{k_a}^{\mathrm{u}} < 1$. The symbol transmitted by the k_a th user is given by $\sqrt{\eta_{k_a}^{\mathrm{u}}} q_{k_a}$ with $\mathbb{E}\left\{\left|q_{k_a}\right|^2\right\} = 1$, is the symbol of k_a th user.

The signal received at the *a*th ARS as

$$\mathbf{y}_a^{\mathrm{u}} = \sqrt{\rho^{\mathrm{u}}} \sum_{a'=1}^{A} \mathbf{g}_{ak_{a'}} \sqrt{\eta_{k_{a'}}^{\mathrm{u}}} q_{k_{a'}} + \mathbf{w}_a^{\mathrm{u}}$$
$$= \sqrt{\rho^{\mathrm{u}}} \hat{\boldsymbol{g}}_{ak_a} \sqrt{\eta_{k_a}^{\mathrm{u}}} q_{k_a} + \sqrt{\rho^{\mathrm{u}}} \varepsilon_{ak_a} \sqrt{\eta_{k_a}^{\mathrm{u}}} q_{k_a} \quad (7)$$
$$+ \sqrt{\rho^{\mathrm{u}}} \sum_{a' \neq a}^{A} \boldsymbol{g}_{ak_{a'}} \sqrt{\eta_{k_{a'}}^{\mathrm{u}}} q_{k_{a'}} + \mathbf{w}_a^{\mathrm{u}},$$

The term $\mathbf{w}_a^{\mathrm{u}}$ represents additive Gaussian noise. In Eq. (7), the first term refers to the desired signal, while the second and third terms correspond to the channel estimation error and interference caused by other users. To calculate the achievable uplink rate for the *k*th user, the uncorrelated effective noise is defined as the sum of the last three terms in Eq. (7). $\mathbf{y}_a^{\mathrm{u}}$ is decomposed into four distinct components as described below

$$\mathbf{y}_a^{\mathrm{u}} = D_a q_{k_a} + C_a q_{k_a} + \sum_{a' \neq a}^{A} I_{aa'} q_{k_{a'}} + \mathbf{w}_a^{\mathrm{u}}, \quad (8)$$

where

$$D_a = \sqrt{\rho^{\mathrm{u}}} \hat{g}_{ak_a} \sqrt{\eta_{k_a}^{\mathrm{u}}},$$
$$C_a = \sqrt{\rho^{\mathrm{u}}} \varepsilon_{ak_a} \sqrt{\eta_{k_a}^{\mathrm{u}}},$$
$$I_{aa'} = \sqrt{\rho^{\mathrm{u}}}\, \mathrm{g}_{ak_{a'}} \sqrt{\eta_{k_{a'}}^{\mathrm{u}}}.$$

Consequently, the uplink rate at the GBS can be determined using the following expression:

$$R_{k_a}^{\mathrm{u}} = log_2 \left(1 + \frac{\|D_a\|^2}{\mathrm{E}\left\{\|C_a\|^2\right\} + \sum_{a' \neq a}^{A} \mathrm{E}\left\{\|I_{aa'}\|^2\right\} + 1} \right) \quad (9)$$

In the proposed framework, the GBS undertakes various functions, including signal reception and demodulation, resource coordination, and the execution of optimization algorithms, among others. As a result, we obtain the closed-form expression for calculating the achievable uplink rate, given in Eq. 10

$$R_{k_a}^{\mathrm{u}} = \mathbb{E}\Big\{ log_2 \left(1 + \frac{\rho^{\mathrm{u}} \eta_{k_a}^{\mathrm{u}} \sum_{m=1}^{M} \left[g_{ak_a}^{*} \right]_m \left[\hat{g}_{ak_a} \right]_m}{M \rho^{\mathrm{u}} \eta_{k_a}^{\mathrm{u}} \left(\beta_{ak_a} - \omega_{ak_a} \right) + M \rho^{\mathrm{u}} \sum_{a' \neq a}^{A} \eta_{k_{a'}}^{\mathrm{u}} \beta_{ak_{a'}} + 1} \right) \Big\} \quad (10)$$

Even though the channel does not exhibit hardening, $\left\| \left[\hat{g}_{ak_a} \right]_m \right\|^2$ follows an exponential distribution with a mean of ω_{ak_a}. Consequently, the uplink rate can be expressed in closed form using the exponential integral function $\mathrm{Ei}(.)$ as

$$R_k^{\mathrm{u}} = -\left(log_2 e \right) e^{\frac{1}{\bar{\omega}_{ak_a}}} \mathrm{Ei}\left(-\frac{1}{\bar{\omega}_{ak_a}} \right), \quad (11)$$

where

$$\bar{\omega}_{ak_a} \triangleq \frac{M \rho^{\mathrm{u}} \eta_{k_a}^{\mathrm{u}} \omega_{ak_a}}{M \rho^{\mathrm{u}} \eta_{k_a}^{\mathrm{u}} \left(\beta_{ak_a} - \omega_{ak_a} \right) + M \rho^{\mathrm{u}} \sum_{a' \neq a}^{A} \eta_{k_{a'}}^{\mathrm{u}} \beta_{ak_{a'}} + 1}. \quad (12)$$

Function Ei(.) is defined at [Eq.(8.211.1)] [16] as follows

$$\mathrm{Ei}\left(x\right) = -\int_{-x}^{\infty} \frac{e^{-t}}{t} dt = \int_{\infty}^{-x} \frac{e^{-t}}{t} dt = \mathrm{li}\left(e^{x}\right)$$

with x < 0.

2.4. Power Optimization

A uniform transmit power allocation for all users is a simplistic approach that introduces several drawbacks. A key issue is the energy consumption of users, especially considering that these users are typically compact, cost-efficient, and highly portable communication units. Moreover, applying the same transmit power across all users exacerbates interference levels, which degrades system efficiency. To overcome these limitations, we propose an uplink power control algorithm utilizing the max-min

power control strategy, which is mathematically formulated as follows

$$\max_{\left\{\eta_{k_a}^{\mathrm{u}}\right\}} \min_{k=1,\ldots,K} R_k^{\mathrm{u}} \quad \theta \le \eta_{k_a}^{\mathrm{u}} \le 1, \quad \forall k = 1,\ldots,K. \tag{13}$$

Since the value of R_k^{u} is a monotonically increasing function of $\bar{\omega}_{a_k k}$. Therefore, (13) is equivalent to

$$(\mathbf{P1}): \max_{\left\{\eta_{k_a}^{\mathrm{u}}\right\}} \min_{k=1,\ldots,K} \bar{\omega}_{a_k k}, \tag{14a}$$

$$\theta \le \eta_{k_a}^{\mathrm{u}} \le 1, \quad \forall k = 1,\ldots,K. \tag{14b}$$

The (P1) problem involves maximizing $\min_{k=1,\ldots,K} \bar{\omega}_{a_k k}$ with respect to the variable η_k^{u}. To solve the (P1) optimization problem, it is essential that the objective function and constraints are either linear or quasi-linear. While Eq. (14a) is a linear function, (14b) does not guarantee linearity. To address this, we reformulate Eq. (14a) by introducing a slack variable t, where t serves as the upper bound of $\min_{k=1,\ldots,K} \bar{\omega}_{a_k k}$ [17]. Consequently, the (P1) problem includes an additional constraint, $t \le \bar{\omega}_{a_k k}$. Hence, the (P1) problem can be reformulated as follows:

$$(\mathbf{P2}): \max_{\left\{\eta_{k_a}^{\mathrm{u}}\right\}, t} t \tag{15a}$$

$$t \le \bar{\omega}_{a_k k}, k = 1,\ldots,K \tag{15b}$$

$$0 \le \eta_{k_a}^{\mathrm{u}} \le 1, k = 1,\ldots,K. \tag{15c}$$

The (P2) problem is a quasi-linear program, which can be effectively solved through the application of the Bisection method [17], as detailed below.

Algorithm 2: Bisection Method

- **Initialization:** Initialize t_{min} and t_{max}, which define the range of possible values for the objective function in (P2). Specify a tolerance value $\epsilon > 0$
- **Solving:** Compute the midpoint $t \leftarrow \frac{t_{min} + t_{max}}{2}$, address the feasibility aspect of the quasi-linear problem in (P2).
- **Update:** If the constraints are satisfied

If feasible, update $t_{min} \leftarrow t$,

If not feasible, update $t_{max} \leftarrow t$.

- **Convergence:** Repeat the process until $t_{max} - t_{min} \le \epsilon$.

At this point, *t* represents the approximate solution to the feasibility problem.

The Bisection method iteratively halves the interval to approximate the optimal value, making it effective for simple functions. Higher accuracy requires a smaller tolerance but increases iterations, leading to greater computational complexity.

Computational complexity: Accuracy of Bisection Algorithm depends on the tolerance level, with lower tolerance improving precision but increasing computational complexity due to more iterations. The required number of iterations to achieve a solution within the tolerance ϵ is given by $n \ge log_2\left(\frac{t_{max} - t_{min}}{\epsilon}\right)$ ensuring convergence and accuracy.

3. Numerical Results and Discussions

We analyze the efficiency of the uplink SC multi-ARS framework by comparing its operation with and without power optimization, considering the influence of various parameters, including the total number of ARSs (*A*), the total number of users (*K*), the number of antennas per ARS (*M*), and and the uplink pilot length $\left(\tau^{\mathrm{p}}\right)$.

Table 1. The system parameters utilized for the simulation.

Parameter	Value
Bandwidth (B)	1.9 GHz
Carrier frequency (f_c)	20MHz
Coherence time $(\mathrm{T_c})$	200 KHz
Coherence bandwidth $(\mathrm{B_c})$	1 ms
The noise figure (NF)	9 db
ARS height	22.5 to 300m
ρ^{p} , ρ^{u}	100, 100 mW
Coherence interval (τ^{c})	200 samples
Area distribution of ARS and users (S)	1 km^2

3.1 Parameters and Setup

The parameters listed in Table 2 are consistently applied across all experiments, similar to those in [11] . ARSs are randomly distributed in 3D space following a continuous uniform distribution over a $1\ km^2$ and the heights range is $22.5m \le h_{ARS} \le 300m$. The distance has been clearly expressed and calculated in the path loss equation of the channel model (LoS-NLoS). ARS selection strategy based on large-scale fading coefficients is used in this model.

For the case without power control: All users communicate at full power, i.e., $\eta_k^{\mathrm{u}} = 1, k = 1,...,K.$

For the case with power control: Each user flexibly controls the transmit power based on the power control coefficient. Coefficients are found according to the algorithm presented previously in Section 3.

In our experiments, we have computed the CDF for the uplink throughput of each user. This has been achieved by implementing the specified scenario.

Limitations: It is important to note that our study introduces a novel model based on the ARS and CF communication framework, while previous research has primarily focused on UAVs either as users or base stations, typically involving only a limited number of UAVs. Given this distinction, our study specifically addresses the power optimization problem without making direct comparisons with other optimization algorithms, aiming to ensure fairness in service quality for all users. In future work, we plan to extend our research by exploring additional optimization methods and alternative ARS selection strategies to further enhance system efficiency and adaptability.

3.2 Results and Discussions

In Fig. 3, we compare the CDF of the per-user uplink throughput with and without uplink power optimization. This comparison is conducted using the parameters *A=15, M=1,* $\tau^{\mathrm{p}} = 10$, and varying the number of users as *K=8, 10, 12.*

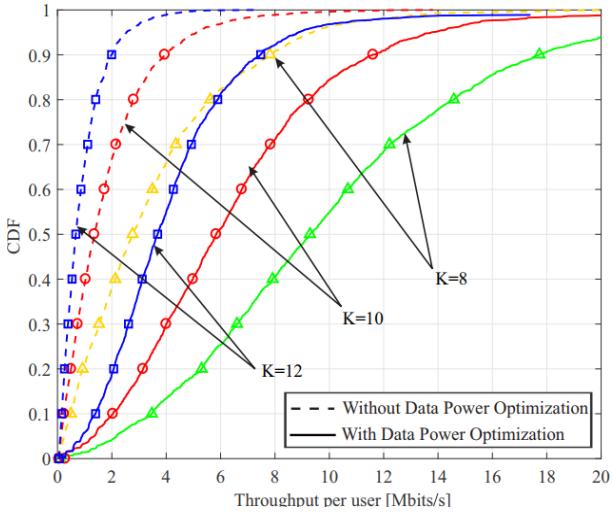

Fig. 3: CDFs of the per-user throughput with/without power optimization, K=8, 10, 12, A=15, M=1, and $\tau^{\mathrm{p}} = 10.$

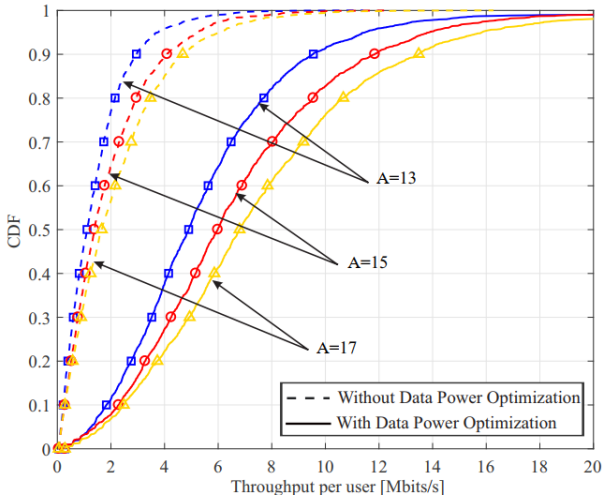

Fig. 4: CDFs of the per-user throughput with/without power optimization, A=13, 15, 17, K=10, M=1, and $\tau^{p}=10$.

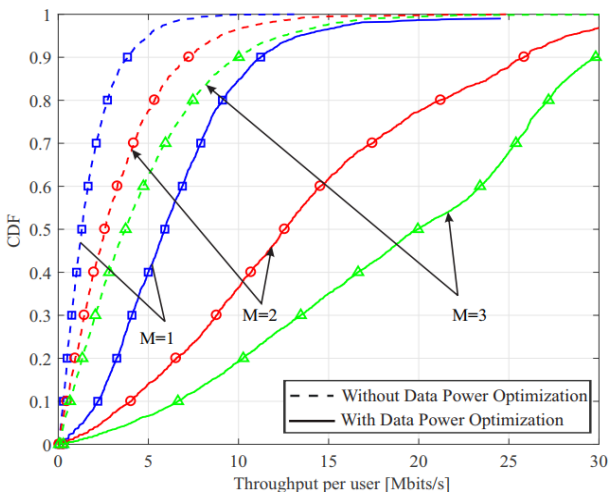

Fig. 5: CDFs of the per-user throughput with/without power optimization, M=1, 2, 3, A=15, K=10, and $\tau^{p}=10$.

It is evident that utilizing power optimization significantly enhances operation compared to the scenario without optimization. For instance, when *K=8*, the 90%-likely per-user throughput with power optimization reaches approximately 3.6 Mbits/s, whereas, without power optimization, it is drastically lower at only 0.4 Mbits/s , representing a ninefold reduction. This disparity arises because, in systems without uplink power control, interference at the receiver is significantly higher.

Additionally, Fig. 3 indicates that operation quality declines as the number of users increases. This is because the evaluation is based on per-user throughput rather than total throughput. When the number of users is small relative to the number of ARSs, users are more likely to experience favorable communication channels, as there are additional alternative paths available to mitigate poor channel conditions.

A similar observation can be drawn from Fig. 4, where the number of ARSs is varied. As A value increases, the options for channel selection become more abundant. This redundancy enhances the likelihood of selecting a favorable channel, thereby improving overall operation.

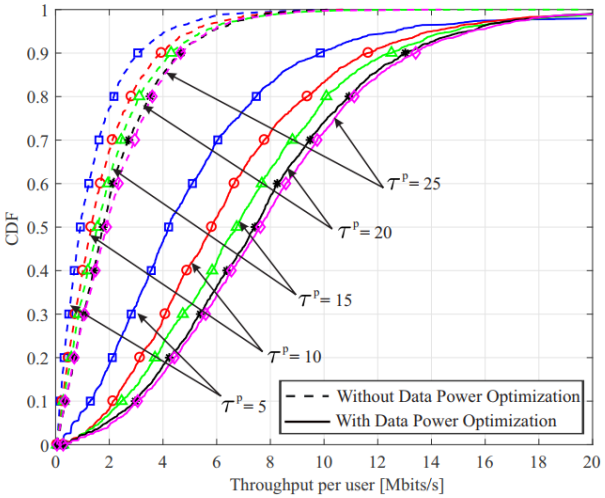

Fig. 6: CDFs of the per-user throughput with/without power optimization, A= 15, K=10, M=1, $\tau^{p}=5,\ 10,\ 15,\ 20,\ 25$.

Fig. 5 illustrates how system performance varies with changes in the number of antennas per ARS (*M*). As the number of antennas increases, the diversity gain improves, resulting in higher throughput. The greater the

number of antennas at each ARS, the more pronounced the performance enhancement. Specifically, as shown in Fig. 5, the improvement in system performance is particularly noticeable when *M=3*.

Finally, the effect of pilot length τ^{p} is illustrated in Fig. 6. Within a certain range, increasing the pilot length improves per-user throughput by providing more accurate channel coefficient estimates. As τ^{p} increases, the number of orthogonal pilots assigned to users also rises, which eliminates pilot contamination. This results in improved channel estimation quality and a reduction in coherent interference. The most significant improvement occurs when τ^{p} increases from 5 to 10. However, beyond this point, further increases in τ^{p} yield only marginal gains. For instance, τ^{p} = 20 and τ^{p} = 25 exhibit nearly identical performance. This occurs because excessively long pilot intervals shorten the uplink data transmission time, ultimately reducing overall data throughput. This issue is visually represented in Fig. 7.

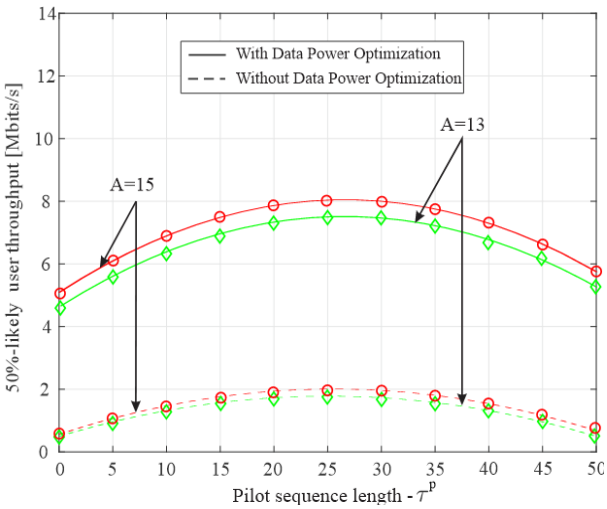

Fig. 7: 50%-likely user throughput versus different pilot sequence length with/without data power optimization, A= 15, K=10, M=1.

Fig. 7 illustrates the trend in 50%-likely user throughput as the channel training duration varies. The per-user throughput reaches its peak at $\tau^{p} = 20$ and subsequently tends to saturate and decrease. The underlying cause of this phenomenon has already been explained in Fig. 6.

4. Conclusion

This paper introduced the Multi-ARS SC model, where ARSs and users were randomly deployed. The proposed model outperformed traditional SC systems with ground-based infrastructure. A power optimization algorithm was implemented, significantly improving efficiency over the non-optimized approach. The study evaluated various scenarios, considering ARS density, antenna count, user distribution, and pilot interval length. ARS-user pairing in the uplink was based on the highest large-scale fading coefficient. While the selection algorithm ensured local optimization, achieving global optimality remained a challenge, highlighting the need for future research on advanced selection methods.

References

1. D. Pliatsios, S. K. Goudos, T. Lagkas, V. Argyriou, A.-A. A. Boulogeorgos, and P. Sarigiannidis, "Drone-base-station for next-generation internet-of-things: A comparison of swarm intelligence approaches," IEEE Open Journal of Antennas and Propagation, vol. 3, pp. 32-47, 2021.
2. B. A. Duc, T. M. Hoang, N. T. Phuong, X. N. Tran, and P. T. Hiep, "Power Optimization and ARSs Selection Strategies in Downlink Cell-Free Multi-ARSs Communication Systems," Arabian Journal for Science and Engineering, pp. 1-18, 2024.
3. M. H. Alsharif and R. Nordin, "Evolution towards fifth generation (5G) wireless networks: Current trends and challenges in the

deployment of millimetre wave, massive MIMO, and small cells," Telecommunication Systems, vol. 64, pp. 617-637, 2017.
4. Y. Pak, K. Min, and S. Choi, "Performance evaluation of various small-cell deployment scenarios in small-cell networks," in The 18th IEEE International Symposium on Consumer Electronics (ISCE 2014), 2014: IEEE, pp. 1-2.
5. J. Chen, X. Ge, and Q. Ni, "Coverage and handoff analysis of 5G fractal small cell networks," IEEE Transactions on Wireless Communications, vol. 18, no. 2, pp. 1263-1276, 2019.
6. J. Tanveer, A. Haider, R. Ali, and A. Kim, "An overview of reinforcement learning algorithms for handover management in 5G ultra-dense small cell networks," Applied Sciences, vol. 12, no. 1, p. 426, 2022.
7. D. C. Nguyen et al., "6G Internet of Things: A comprehensive survey," IEEE Internet of Things Journal, vol. 9, no. 1, pp. 359-383, 2021.
8. B. Li, S. Zhao, R. Miao, and R. Zhang, "A survey on unmanned aerial vehicle relaying networks," IET communications, vol. 15, no. 10, pp. 1262-1272, 2021.
9. K. Messaoudi, O. S. Oubbati, A. Rachedi, A. Lakas, T. Bendouma, and N. Chaib, "A survey of UAV-based data collection: Challenges, solutions and future perspectives," Journal of network and computer applications, vol. 216, p. 103670, 2023.
10. M. A. Ouamri, D. Singh, M. A. Muthanna, A. Bounceur, and X. Li, "Performance analysis of UAV multiple antenna-assisted small cell network with clustered users," Wireless Networks, vol. 29, no. 4, pp. 1859-1872, 2023.
11. B. A. Duc, T. M. Hoang, N. T. Phuong, X. N. Tran, and P. T. Hiep, "Optimizing power for data transmissions in uplink cell-free multi-ABSs communication systems," in 2022 International Conference on Advanced Technologies for Communications (ATC), 2022: IEEE, pp. 23-28.
12. B. A. Duc, T. M. Hoang, N. T. Phuong, X. N. Tran, and P. T. Hiep, "Pilot and data power optimization problems in multiple Aerial Relay Stations cell-free communication systems," International Journal of Communication Systems, vol. 37, no. 10, p. e5765, 2024.
13. 3GPP, "Technical specification group radio access network; study on enhanced LTE support for aerial vehicles," TR 36.777, Dec 2017.
14. H. Q. Ngo, A. Ashikhmin, H. Yang, E. G. Larsson, and T. L. Marzetta, "Cell-free massive MIMO versus small cells," IEEE Transactions on Wireless Communications, vol. 16, no. 3, pp. 1834-1850, 2017.
15. S. K. Sengijpta, "Fundamentals of statistical signal processing: Estimation theory," ed: Taylor & Francis, 1995.
16. I. S. Gradshteyn and I. M. Ryzhik, Table of integrals, series, and products. Academic press, 2014.
17. E. K. P. L. Chong, Wu-Sheng / Żak, Stanislaw H., An introduction to optimization 4th. John Wiley & Sons, 2023.